PCR-based survey of methane-cycling archaea in methane-soaked subsurface sediments of Guaymas Basin, Gulf of California

John E. Hinkle[1], Paraskevi Mara[2], David Beaudoin[2], Virginia P. Edgcomb[2], Andreas P. Teske[1]

[1]Department of Earth, Marine and Environmental Sciences, University of North Carolina at Chapel Hill, Chapel Hill, North Carolina, USA

[2]Department of Geology and Geophysics, Woods Hole Oceanographic Institution, Falmouth, Massachusetts, USA

Corresponding authors:

John E. Hinkle (jehinkle@unc.edu)

Andreas P. Teske (teske@email.unc.edu)

Running Head: Guaymas Basin Subsurface Methane-Cycling Archaea

Abstract. The Guaymas Basin in the Gulf of California is characterized by active seafloor spreading, rapid deposition of organic-rich sediments, steep geothermal gradients, and abundant methane of mixed thermogenic and microbial origin. Subsurface sediment samples were selected from eight drilling sites to explore the diversity, depth range, and in-situ temperature range of methane-cycling archaea in the Guaymas Basin subsurface, using PCR amplification with general (mcrIRD) and ANME-1 specific primers targeting the alpha (α) subunit of methyl coenzyme M reductase, encoded by the *mcrA* gene. Diverse ANME-1 lineages were detected in seven drilling sites, preferentially around the methane-sulfate interface, and in several cases showed preferences for specific sites and types of sediment. Phylogenetically, most ANME-1 sequences from the Guaymas Basin subsurface were related to similar sequences from marine mud volcanoes, seep sites, and the shallow marine subsurface. Methanogenic lineages were found in three sites. The most frequently recovered phylotypes, closely affiliated with the hyperthermophilic *Methanocaldococcaceae*, were found at the hydrothermally influenced Ringvent site. The coolest drilling site, in the northern axial trough of Guaymas Basin, yielded the greatest diversity of methanogen lineages. Our survey indicates extensive microbial methane cycling within subsurface sediments of Guaymas Basin, and calls attention to deep sources of thermogenic methane where potential microbial processing remains to be shown.

Importance. The Guaymas Basin has received significant attention from microbiologists and biogeochemists due to the abundance of methane in its sediments. This study has identified new ANME-1 and methanogenic lineages and phylogenetic clusters present in subsurface Guaymas Basin sediments. Our work allows for a greater understanding of 1) the diversity of methane-cycling archaea and 2) methane-cycling in the Guaymas Basin.

Keywords. Guaymas Basin, ANME-1, methanogens, phylogenetics, methane, *mcrA*

INTRODUCTION

The Guaymas Basin is a young marginal rift basin in the Gulf of California characterized by active seafloor spreading, volcanic sill intrusions into rapidly deposited organic-rich sediments, and steep geothermal gradients where sedimentary organic material of photosynthetic origin turns into hydrocarbons, which can potentially be utilized by microbes as substrates. The dominant hydrocarbon in Guaymas Basin sediments, methane, is of predominantly thermogenic origin in the hot subsurface and gradually changes to microbially produced methane in the upper, cooler sediments (Simoneit et al., 1986, Teske et al., 2019, Bojanova et al., 2023).

Using seafloor samples collected by submersible, hyperthermophilic methanogens (*Methanocaldococcus*, *Methanopyrus*) have been isolated from hydrothermal hot spots in the southern axial trough of Guaymas Basin (Jones et al. 1983, Kurr et al. 1991). PCR-based surveys have detected a wide range of methanogenic lineages in surficial Guaymas Basin sediments (Dhillon et al., 2005, Lever and Teske, 2015), including members of the obligately methylotrophic Methanofastidiosa lineage (Nobu et al., 2016). Sulfate-dependent anaerobic methane-oxidizing archaea (predominantly ANME-1 and ANME-2) are widespread in surficial sediments of Guaymas Basin (Teske et al., 2002, Biddle et al., 2012, Dowell et al., 2016, McKay et al., 2016). Thermophilic ANME-1 lineages were enriched from hydrothermal sediments of Guaymas Basin at temperatures ranging from 50 to 70°C (Holler et al. 2011, Wegener et al. 2015, Benito-Merino et al. 2022), and at 70°C from Pescadero Basin in the southern Gulf of California (Speth et al. 2022, Laso-Pérez et al. 2023).

In contrast to the well-studied surficial sediments of Guaymas Basin, investigations into the diversity and activity of methane-cycling microorganisms in the sedimentary subsurface of Guaymas Basin are just beginning. Enrichments from subsurface sediments obtained during DSDP

Expedition 64 demonstrated viable methanogens within the upper 20 m of the sediment column (Oremberg et al., 1982). High-throughput 16S rRNA gene sequencing surveys of the shallow Guaymas Basin subsurface, down to 5 m sediment depth, detected mainly ANME-1 archaea, and found only traces of diverse methanogen lineages (Teske et al., 2019). The scarcity of methanogens was also noted by a recent metagenomic study of deep subsurface sediments in Guaymas Basin (Bojanova et al., 2023).

To examine the diversity and distribution of methanogens and methane-oxidizing archaea with a targeted key gene approach, we performed PCR amplification and sequencing of the *mcrA* gene, which encodes the alpha (α) subunit of methyl coenzyme M reductase that catalyzes the final step of methanogenesis. During this step, the cofactor-bound methyl group is reduced and released as methane. This enzyme also works in reverse, catalyzing sulfate-dependent methane oxidation by methane-oxidizing archaea (Thauer, 2019). Since *mcrA* genes are diagnostic for methane-cycling archaea, they serve as a specific alternative and complement to 16S rRNA genes for the phylogenetic analysis of methane-cycling archaea (Luton et al., 2002, Hallam et al., 2003). Previous 16S rRNA and *mcrA*-based surveys of surficial Guaymas sediments yielded diverse methanogens and methane-oxidizers, using general and group-specific PCR primers (Lever and Teske, 2015). Here we use the partial *mcrA* gene sequences to construct phylogenetic trees for a detailed study of methane-cycling archaeal diversity in deep subsurface Guaymas sediments that were sampled during International Ocean Discovery Program (IODP) expedition 385 (Teske et al., 2021a).

RESULTS

Site characteristics. PCR-amplified *mcrA* genes were obtained from nearly all drilling sites of IODP Expedition 385 (Fig. 1) which differ in their degree of hydrothermally driven heat flow (Neumann et al., 2023), and in the relative extent of marine vs terrestrial sedimentation (Persad and Masaglia, 2023). Samples yielding PCR amplicons were generally affiliated with subsurface maxima or with broad zones of high alkalinity and DIC concentration (Torres and Kim 2022), a proxy for microbial organic matter remineralization (Supplementary Figures S1 and S2). Sediment samples, DNA yields, and PCR results are summarized in Table 1. Two neighboring sites (U1545 and U1546) on the northwestern end of Guaymas Basin (Teske et al., 2021b,c) essentially differ by the presence of a massive, thermally equilibrated sill between 350 to 430 meters below seafloor (mbsf) at Site U1546 (Lizarralde et al., 2023). Two drilling sites (U1547, U1548) at the hydrothermally active Ringvent area, approximately 28 km northwest of the spreading center (Teske et al. 2019) target a shallow, recently emplaced, hot sill that creates steep thermal gradients and drives hydrothermal circulation (Teske et al. 2021d). Site U1549 (Teske et al. 2021e) samples the periphery of an off-axis methane cold seep, Octopus Mound, located ~9.5 km northwest of the northern axial graben. Site U1550 is located close to DSDP site 481 and samples the heterogonous (marine and terrestrial) sediments that are accumulating in the northern axial valley (Teske et al. 2021f). Site U1551 represents the terrestrially influenced sediments of the southeastern Guaymas Basin with riverine sand input from the Yaqui River (Teske et al. 2021g). Site U1552 (Teske et al. 2021h) sampled the subsurface of a cold seep site surrounded by shallow methane hydrates, close to the Sonora Margin.

Regarding their in-situ temperature gradients, the Guaymas Basin drilling sites fall into two categories, the hot Ringvent sites with steep temperature gradients of ca. 50 to 100°C/100 m

depth, and the majority of Guaymas sites with elevated temperature gradients of approx. 20 to 25°C/100 m (Fig. 2). Even the gradient at the coolest site, U1550 with ca. 13-14°C/100m, is at least twice as steep as the temperature gradients commonly found for ocean crust. These distinct thermal gradients are to some extent reflected in different lineages of detected methanogens.

Detection of Methanogen lineages. Three of the seven examined sites (U1547B, U1548B, and U1550B) yielded *mcrA* genes related to previously established methanogens or methane-cycling archaea, using PCR primers that were modified to encompass the widest possible diversity of *mcrA* genes, but do not capture ANME-1 (Lever and Teske, 2015).

Two sites (U1547B and U1548B) are located at the Ringvent mound, an off-axis hydrothermal system driven by recent sill emplacement (Fig. 3). Here, the temperature gradients increase rapidly along a sampling transect with tightly spaced, increasing temperature measurements towards the "Ring of Fire" (Fig. 2) where conspicuous hydrothermal activity and a topographical high of ca. 20 m mark the top rim of the buried sill (Teske et al. 2019). At Ringvent sites U1547B and U1548B, the most abundant phylotypes were close relatives of the extreme hyperthermophile and obligate hydrogenotroph *Methanocaldococcus bathoardescens* (Fig. 4), originally isolated from low-temperature hydrothermal fluid (26°C) at the Axial Seamount on the Juan de Fuca Ridge (Stewart et al., 2015). Although isolated from relatively temperate fluids, *Methanocaldococcus bathoardescens* is a hyperthermophile that grows under temperatures from 48 to 90°C, with a thermal optimum of 82°C (Stewart et al., 2015). Samples from the Ringvent mound sites also yielded *mcrA* genes of the *Methanosarcinaceae* (capable of using acetate, CO_2, and methyl substrates for methanogenesis) and the mostly hydrogenotrophic *Methanomicrobiaceae* (Fig. 4).

At the cool axial site, U1550B, greater methanogenic diversity was observed, including the obligately acetoclastic *Methanosaetaceae*, the metabolically diversified *Methanosarcinaceae*, and the most hydrogenotrophic or (occasionally) ethanol-utilizing *Methanomicrobiaceae* and *Methanobacteraceae* (Fig. 4). Additionally, the uncultured *mcrA* "group E" lineage related to anaerobic methane-oxidizing ANME archaea (Hallam et al. 2003), and an uncultured Guaymas group without any cultured relatives were detected at this site (Lever and Teske, 2015).

ANME-1 diversity. While methanogen populations were only observed at three sites (U1547B, U1548B, and U1550B), seven sites (all except U1546B) yielded *mcrA* gene sequences affiliated with the ANME-1 lineage (Methanophagales), using primers fine-tuned for this order-level lineage (Lever and Teske, 2015). Extensive GenBank searches and comparisons to database sequences showed that ANME-1 phylotypes from Guaymas Basin subsurface samples were closely related to reference sequences from the Napoli mud volcano (Lazar et al., 2011), from subsurface sediments of the Mississippi Canyon 118 seep site in the Gulf of Mexico (Underwood et al., 2016), and from shallow subsurface sediments recovered by piston coring and push coring in Guaymas Basin (Teske et al. 2019, Teske et al. 2021i). Almost all ANME-1 *mcrA* gene sequences could be accommodated in sixteen distinct phylogenetic clusters (Figure 5). These clusters were further examined and confirmed through site-specific *mcrA* gene phylogenies for five sites, U1547B, U1548B, U1550B, U1551B, and U1552B (Supplementary Figures S3 to S7).

In searching for thermophilic ANME-1 lineages, we found that cluster VIII, consisting of *mcrA* genes from ANME-1 enrichments in surficial sediments at 50ºC (Holler et al. 2011), also included Guaymas subsurface *mcrA* genes from site U1551B. However, we observed no overlap of Guaymas subsurface *mcrA* genes with *mcrA* genes from 70ºC methane-oxidizing ANME-1 enrichment cultures (Benito-Merino et al., 2022, Laso-Pérez et al., 2023).

Habitat and site preferences of different *mcrA* gene lineages were visualized with a bubble plot of *mcrA* gene recovery, color-coded by habitat type (Fig. 6, and Supplementary Figure S8). From the relatively cool northwestern site: U1545B, only a single sample yielded *mcrA* gene sequences, all of them members of cluster 3 (color-coded in grey). Gene sequences from the hydrothermal Ringvent sites (in red, Fig. 6) were highly diverse, and affiliated with clusters 1, 2, 5, 6, 10. 11, 12, 14, 15 and 16. Gene sequences from the axial site U1550B were also diverse (color-coded in green, Fig. 6). Gene sequences from the terrestrially influenced site U1551B were largely affiliated with group 13 (Fig. 5), plus smaller proportions of U1551B-derived sequences that fell into clusters 1, 3, 8 and 10 (Fig. 6). Cluster 13, which dominated the samples from site U1551, did not include any sequences from other sites and thus provides the best example, within this dataset, for strong habitat preference within a particular lineage (color-coded in brown, Fig. 6). GenBank searches for published *mcrA* genes that would be falling into this cluster remained unsuccessful. Finally, gene sequences from the cold seep site U1552B were affiliated with clusters 3, 7, and 9 (color-coded in blue, Fig. 6).

DISCUSSION

ANME-1 diversity. The methane-oxidizing group, ANME-1, is widespread in the Guaymas Basin, as it was observed at every site examined, particularly near depths where methane-sulfate interfaces occur. Methane-sulfate interfaces are present at varying depths in the subsurface, depending on geologic formations and methane flux. To some extent, the different regions in the Guaymas Basin are characterized by different ANME-1 types. While it is possible that some clades may not be detected due to sensitivity issues or sequencing artifacts, our data identify clades that show an observable preference for particular sites, which differ in temperature

and geochemistry. This differentiation can be observed by comparing the clusters in the phylogenies constructed specifically for each drilling site. For example, when comparing the Site U1548B and U1552B phylogenies, the phylogeny of methane hydrate Site 1552B contains three distinct ANME-1 clusters, two of which are not shared with the phylogeny of hydrothermally influenced Ringvent Site U1548B (Figs. S4 & S8 in the supplemental material). These differences in ANME-1 cluster representation across sites suggest how the locally distinct thermal profiles (Fig. 2) and in-situ temperature conditions contribute to shaping the microbial biogeography of the Guaymas Basin.

Mud volcano connection. Close phylogenetic relationships between sequences from mud volcano and deep subsurface sediments were observed in the general ANME-1 phylogeny (Fig. 5). Previous research indicates that these similarities reflect the role of mud volcanoes as a "window to the deep subsurface", dispersing microbes from the deep subsurface into the hydrosphere; as mud volcanoes erupt, they bring gas-rich fluidized sediment and its microbial populations from the deep subsurface to the seafloor (Rattray et al., 2022). Mud volcanoes could garner more attention as an alternative way to study the deep marine biosphere since R/V *JOIDES Resolution* will be decommissioned in October 2024 and plans for a replacement vessel have been paused (NSF Announcement, March 31st, 2023) for a prolonged period.

Hyperthermophilic methanogens at Ringvent. Hyperthermophilic methanogens (family *Methanocaldococcaceae*) were not recovered from deep, hot sediments, but were recovered from shallow, cool, and relatively oxidizing (sulfate-reducing) sediment samples at 2-3 mbsf in the Ringvent area. This apparent paradox can be explained by the local environmental regime: The Ringvent mound is underlaid by a hot volcanic sill, which drives hydrothermal circulation at the relatively thinly sedimented surface of the mound, and brings hot hydrothermal fluids (up to 75

ºC) to the sediment surface (Teske et al., 2019). Hyperthermophiles could rise with methane-rich hydrothermal fluids from deeper sediments, or may originate from localized hydrothermal hot spots that have been observed at the sediment/water interface of Ringvent (Teske et al. 2019). Either way, hydrothermal circulation could deposit microbial cells in the wider Ringvent area and seed cool, surficial sediments with hyperthermophiles. Previous studies have detected thermophilic methanogen lineages in cool, surficial Guaymas Basin sediments, and have proposed transport to the surface via hydrothermal flow (Dhillon et al., 2005).

Methanogen scarcity. Many ANME-1 sequences were collected from our sampling sites; however, methanogen sequences were relatively scarce. This poses a question: Why are ANME-1 so abundant, yet methanogens so rare in the Guaymas Basin deep subsurface?

While methodological limitations, such as PCR primer range and sensitivity, could play a role, methanogen scarcity is not only observed in this *mcrA* gene survey, but also in 16S rRNA analyses (Teske et al., 2019, McKay et al., 2016), in metagenomic investigations (Bojanova et al., 2023), and in cultivation studies (Castro et al., 2021). It seems unlikely that these conceptually and technically distinct methods are consistently biased against methanogens, and to such a degree that they would miss a large swath of methanogenic diversity. While undetected, “exotic” methanogenic lineages cannot be excluded with certainty, they would have to hide in plain sight (for example, in poorly-described phylogenetic lineages) to comprise a significant portion of methanogenic diversity.

The likely scarcity of methanogens in the Guaymas Basin deep subsurface has implications for the origin and microbial processing of subsurface methane. Methane clumped isotope measurements show that the proportion of biogenic methane increases towards the sediment surface, whereas methane in deep, hot sediments is predominantly thermogenic (Bojanova et al.,

2023). If the population density of active methanogens in the Guaymas subsurface sediments is relatively low, the massive reservoir of biogenic subsurface methane must have accumulated over geological time (Bojanova et al., 2023). Methanogenic gene expression is predominately observed in surficial sediments where most methane-cycling occurs (Mara et al., 2023). Some of this methane produced in surficial sediments could be incorporated into the subsurface reservoir of biogenic methane.

Thermal preferences of methanogens. Notably, the cooler axial site (U1550B) exhibits greater methanogenic diversity than the much warmer Ringvent mound sites (U1547B and U1548B). This difference in diversity may reflect the methanogens' general preference for moderate temperatures (McKay et al., 2016). While thermophilic methanogenic lineages have been isolated from deep-sea vent systems (Jones et al., 1983, Stewart et al., 2015), most cultured methanogenic lineages are not thermophilic (Liu and Whitman, 2008). Observing greater methanogenic diversity in cooler sediments of the Guaymas subsurface underscores the linkage between sediment depth/temperature and methane origin, by supporting the observation that biogenic methane predominates in shallower, cooler sediments, whereas thermogenic/abiotic methane predominates in deeper, warmer sediments (Bojanova et al., 2023).

Future directions. A future direction of this research lies in investigating the matching 16S rRNA datasets and pulling *mcrA* genes from entire genomes. *mcrA* genes pulled from previously published genomes will allow for the strengthening of our current *mcrA* phylogenies. The construction of 16S rRNA phylogenies to complement the existing *mcrA* phylogenies will allow for a comprehensive PCR-based survey of methane-cycling microbial communities in the Guaymas Basin subsurface. Additionally, there is the possibility of linking our *mcrA*-based phylogenies to genome-based phylogenies of ANME-1 (Laso-Pérez et al., 2023).

Another research direction focuses on the volcanic sills of Guaymas Basin. Current research suggests that the abundance of methane located at and in these sills is of predominately thermogenic origin, resulting from the thermal maturation of organic matter (Teske et al., 2021d, Bojanova et al., 2023, Simoneit et al., 1986). However, these sills are known to harbor sediment intrusions, which could contain microbes, and even methanogens. The sediment-sill interfaces remain within the temperature range for methanogenic hyperthermophiles (Kurr et al., 1991). While it is unknown if there is enough accessible energy to support cellular metabolism, sill intrusion contributes to the thermal maturation of organic matter and provides a potential influx of low-molecular weight maturation products that would be available for microbial metabolism (Wellsbury et al., 1997, Lin et al., 2017). Future metagenomic analyses of recovered veined rock samples will seek to address this issue.

METHODS

Sampling. Drilling sites were visited and sampled by R/V *JOIDES Resolution* during Expedition 385 of the International Ocean Discovery Program to Guaymas Basin (15 September–15 November 2019). The off-axis flanking regions and the northern axial trough of Guaymas Basin were targeted to explore the diversity, depth range, and in-situ temperature range of methane-cycling archaea in the Guaymas Basin subsurface. In the targeted regions, eight drilling sites were selected (Fig. 1) and probed by *mcrA* gene amplification and sequencing down to 170 meters below seafloor (Table 1). Sediment cores were collected, split into smaller sections, and frozen at -80 ºC by the shipboard science crew.

Thermal profiles. The Advanced Piston Corer Temperature Tool (APCT-3, Heesemann et al., 2006) and Sediment Temperature Tool (SET-2) were used to measure downhole equilibrium

temperatures. The SET-2 tool was used for temperature measurements in lithified sediments that were too stiff for the APCT-3 tool. The SET-2 tool was only used when necessary as it can lead to cracks in the sediment. These cracks lead to temperature measurements of diminished quality. For a detailed protocol of the downhole temperature measurements, refer to Section 3.2 in Neumann et al, 2023. Temperature values were interpolated for each sample using linear regression of the local thermal gradient (°C/m) multiplied by depth (mbsf), plus the y-axis intercept: U1545A,B, T = 0.225 x depth + 4.899; U1546A, T = 0.221 x depth + 2.627; U1547A/B, T = 0.511 x depth + 13.01; U1548A, T = 0.646 x depth + 8.301; U1548B, T = 0.804 x depth + 6.5; U1548C, T = 0.958 x depth + 15.916; U1548D/E, T = 0.271 x depth + 3.241; U1549A, T = 0.194 x depth + 3.228, U1550A, T = 0.135 x depth + 3.532; U1551A, T = 0.1 x depth + 4.741; U1552A/B, T = 0.262 x depth + 3.543.

DNA extraction. DNA was extracted from near-surface (0.7-2.1 mbsf), intermediate (15.4-54.8 mbsf), and deeper locations (65.7-142 mbsf), as summarized in Table 1. The MP Biomedical FastDNA™ SPIN Kit was used to extract DNA following manufacturer suggestions. Prior to DNA extraction, sediment samples were removed from -80 ^{o}C and were thawed on ice. A subsample of 0.5 gr homogenized sediment was transferred using autoclaved and ethanol-rinsed metallic spatula into sterile, DNA/RNA-free 2 ml tubes containing beads, provided by the manufacturer. All DNA extractions were performed in a UV-sterilized clean hood (two UV cycles of 15 min each) that was installed with HEPA filters. Surfaces inside the hood and pipettes were thoroughly cleaned with RNase AWAY (Thermo Scientific), and with absolute ethanol (200 proof; purity ≥ 99.5%; Thermo Scientific Chemicals) before every extraction and in between extraction steps.

PCR assays and *mcrA* gene analysis. PCR reactions were performed with *mcrA*-targeting primer sets reported to successfully amplify *mcrA* gene sequences of diverse archaeal methane-cycling lineages identified in Guaymas surficial sediments (Lever and Teske, 2015). For our subsurface samples, we used the general mcrIRD primers that cover a range of known *mcrA* gene sequences in Guaymas Basin (F: 5′-TWYGACCARATMTGGYT-3′; R: 5′-ACRTTCATBGCRTARTT-3′), and the ANME-1-specific *mcrA* gene primers (F: 5′-GACCAGTTGTGGTTCGGAAC-3′; R: 5′-ATCTCGAATGGCATTCCCTC-3′) that specifically target the ANME-1 lineage involved in methane cycling in Guaymas (Lever and Teske, 2015). The PCR reactions were performed in triplicate using Takara SpeedSTAR HS DNA polymerase kit (Takara Bio USA, Madison, WI) with the following modifications: each 25 µl reaction contained : each 25 µl reaction contained 0.5-1 ng of template DNA, 2× Takara SpeedSTAR Buffer I, 2.5 mM dNTPs (TaKaRa Bio USA, Madison, WI), 2 µM of each primer (final concentrations), 1.25 units of SpeedSTAR HS DNA Polymerase and DEPC water (Fisher BioReagents) . These reactions were performed at 95°C for 5 min, followed by 35 cycles of 95°C (30 s), 48°C (30 s), and 72°C (45 s) for the mcrIRD primers. The same PCR conditions were also applied for ANME-1-specific *mcrA* primers with the exception that the annealing temperature for this primer was set at 60ºC (30 s). To confirm absence of contamination due to handling and PCR reagents, we included negative controls (blanks) in all PCR experiments, where template DNA was substituted with DEPC water.

2 µl of all PCR amplified samples were run on 2% agarose gel (Low-EEO/Multi-Purpose/Molecular Biology Grade Fisher BioReagents) to verify the amplification of the *mcrA* genes (PCR bands ~ 500 bp in size). As positive control we used DNA from surficial Guaymas sediments collected with Alvin push cores during the AT-4205 research cruise in Guaymas Basin

(Ramírez et al., 2021). Controls were treated as samples for both DNA extractions and PCR amplifications (no sample added). All successful PCR reactions per sample (n=3) were pooled together, and were purified and concentrated using the Agencourt AMPure XP protocol (Beckman Coulter) following the manufacturer's suggestion. The purified/concentrated PCR products were sequenced at Georgia Genomics and Bioinformatics Core (University of Georgia) using the MiSeq Illumina Platform.

The paired reads generated with MiSeq were quality checked and trimmed using FastQC (v. 0.11.7). We analyzed the *mcrA* data using the QIIME2 platform (Bolyen et al., 2019), and the DADA2 plugin provided in the QIIME2 pipeline to denoise and optimize the merging of the forward and reverse reads. The functional annotation of the generated *mcrA* sequences was assigned manually using BLASTX against GenBank NR. The *mcrA* and ANME-1 *mcrA* sequences retained were those that were functionally annotated as "methyl CoM reductase" and presented *e* value scores ≥ 1e-10. Those manually curated sequences that were functionally misannotated were excluded from downstream analysis.

***mcrA* gene phylogeny**. *mcrA* gene sequences were aligned using Multiple Sequence Comparison by Log-Expectation (MUSCLE) in MEGA11. The aligned sequences were used in MEGA11 to construct minimum evolution phylogenetic trees checked by 1000 bootstrap replicates. Bootstrap values indicating greater than 50% support for an individual cluster were included in each phylogenetic tree. For easy reference, all *mcrA* gene sequences in our phylogenetic trees are included in the supplementary materials.

Nucleotide BLAST search (BLASTn) was used to find closely related sequences in NCBI GenBank. These closely related sequences were then included in the trees to add phylogenetic context and allow for cluster labeling. A phylogenetic tree was constructed using the five most

abundant ANME-1 *mcrA* gene sequences from seven of the eight drilling sites. *mcrA* gene sequences from methanogenic lineages were placed into a separate phylogeny. To obtain a wider view of ANME-1 diversity, site-specific trees were constructed for sites where the number of sequences recovered was conducive to constructing a phylogenetic tree. For each site, all sequences with >100 clones were used to construct a phylogenetic tree. An exception was for the site U1550B specific tree which had 200 sequences with >100 clones. For this site, the top 25 sequences, by clone number, from samples 1550B_ 1H2, 1550B_3H2, and 1550B_7H2, (2.0, 16.9, and 54.8 mbsf, respectively; Table 1) along with two sequences from sample 1550B_ 19X2 (142 mbsf) were used to construct a phylogenetic tree.

DATA AVAILABILITY

All *mcrA* generated sequences were deposited into the National Center for Biotechnology Information (NCBI) Sequence Read Archive database under project BioProject ID PRJNA909197 (Biosample accession numbers SAMN33424330 to SAMN33424350). The accession numbers for the *mcrA* sequences from samples 1550B_7H2, 1548B_2H3, and 1547B_2H2 are SRR23604134, SRR23604145, and SRR23604146 respectively. The accession number for the ANME-1 *mcrA* sequences from sample 1545B_4H3 is SRR23604132. The accession number for the ANME-1 *mcrA* sequences from samples 1547B_8H2 and 1547B_9H2 are SRR23604131 and SRR23604130, respectively. The accession numbers for ANME-1 *mcrA* sequences from samples 1548B_1H2, 1548B_2H3, 1548B_3H4 and 1548B_9H3 are SRR23604129, SRR23604128, SRR23604127 and SRR23604126, respectively. The accession number for the ANME-1 *mcrA* sequences from sample 1549B_6H3 is SRR23604144. The accession numbers for ANME-1 *mcrA* sequences from samples 1550B_1H2, 1550B_3H2, 1550B_7H2 and 1550B_19X3 are SRR23604143, SRR23604142, SRR23604141 and SRR23604140, respectively. The accession numbers for ANME-1 mcrA sequences from samples 1551B_1H1, 1551B_2H2, 1551B_3H2 and 1551B_5H2 are SRR23604139, SRR23604138, SRR23604137 and SRR23604136, respectively. The accession numbers for ANME-1 mcrA sequences from samples 1552B_1H2 and 1552B_3H3 are SRR23604135 and SRR23604133, respectively.

ACKNOWLEDGMENTS

Sampling in Guaymas Basin and post-cruise research in the Teske lab was supported by the International Ocean Discovery Program. We thank David Geller-McGrath for an early version of Figure 6. This study was supported by NSF Grant OCE-2046799 to VE, PM, AT, and R.

Hatzenpichler, and by NSF grant OCE-1829903 to VE, PM, and AT. Current research in the Teske lab is supported by NASA Exobiology grant 512580 and by NSF Biological Oceanography grant 5120047.

Table 1. Samples and PCR results for Guaymas Basin subsurface sediments. Sample depths are noted as meters below seafloor (mbsf). The (+) and (-) symbols indicate successful PCR (+), and no PCR (-) amplifications. A version of this table that includes all samples where PCR amplification was attempted can be found in the supplementary materials as Supplementary Table 1.

Site	Sample ID	Depth (mbsf)	T (ºC)	*mcrA* ANME-1 specific primers	*mcrA* general primers (mcrIRD)
U1545B	1545B_1H2	1.7	5.3	—	—
	1545B_4H3	25.8	10.7	+	—
U1547B	1547B_2H2	8.7	17.5	—	+
	1547B_8H2	65.7	46.6	+	—
	1547B_9H2	74.3	51.0	+	—
U1548B	1548B_1H2	2.1	8.2	+	—
	1548B_2H3	8.9	13.7	+	—
	1548B_3H4	20.4	22.9	+	+
	1548B_9H3	76.5	68.0	+	—
U1549B	1549B_6H3	45.6	12.1	+	—
U1550B	1550B_1H2	2.0	3.8	+	—
	1550B_3H2	16.9	5.8	+	—
	1550B_7H2	54.8	10.9	+	+
	1550B_19X2	142.0	22.7	+	—
U1551B	1551B_1H1	0.8	4.8	+	—
	1551B_2H2	5.8	5.3	+	—
	1551B_3H2	15.4	6.3	+	—
	1551B_5H2	34.2	8.2	+	—
U1552B	1552B_1H2	0.8	3.8	+	—
	1552B_3H3	19.2	8.6	+	—

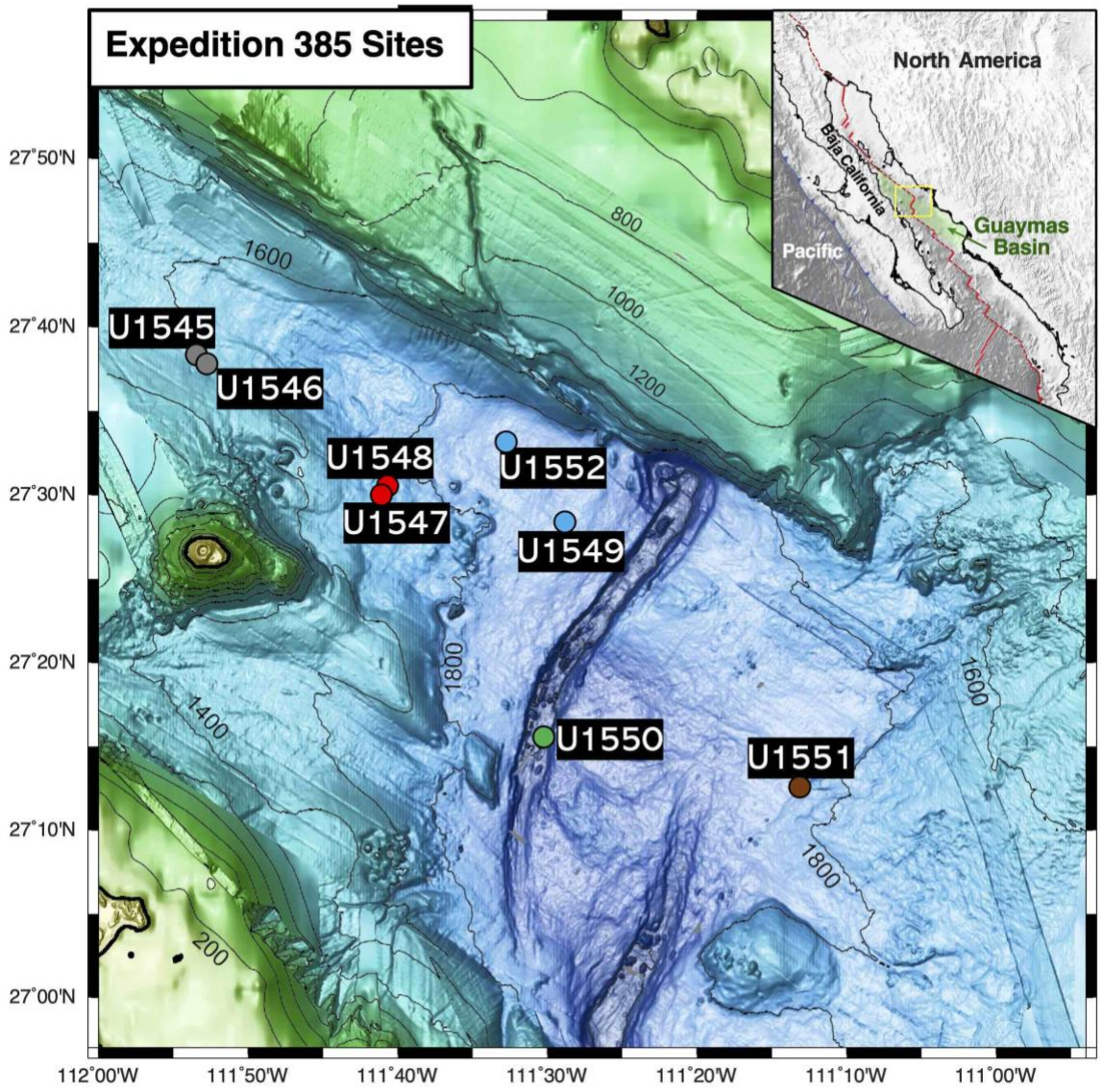

Figure 1. Guaymas Basin drilling site map. The sites follow broadly a northwest-to-southeast transect across the northern Guaymas axial valley. Grey, northwestern off-axis sites U1545 and U1546; red, hydrothermally active Ringvent sites U1547 and U1548; Blue, cold seep sites U1549 and U1552; green, northern Trough axial site U1550; brown, southeastern terrestrially influenced site U1551.

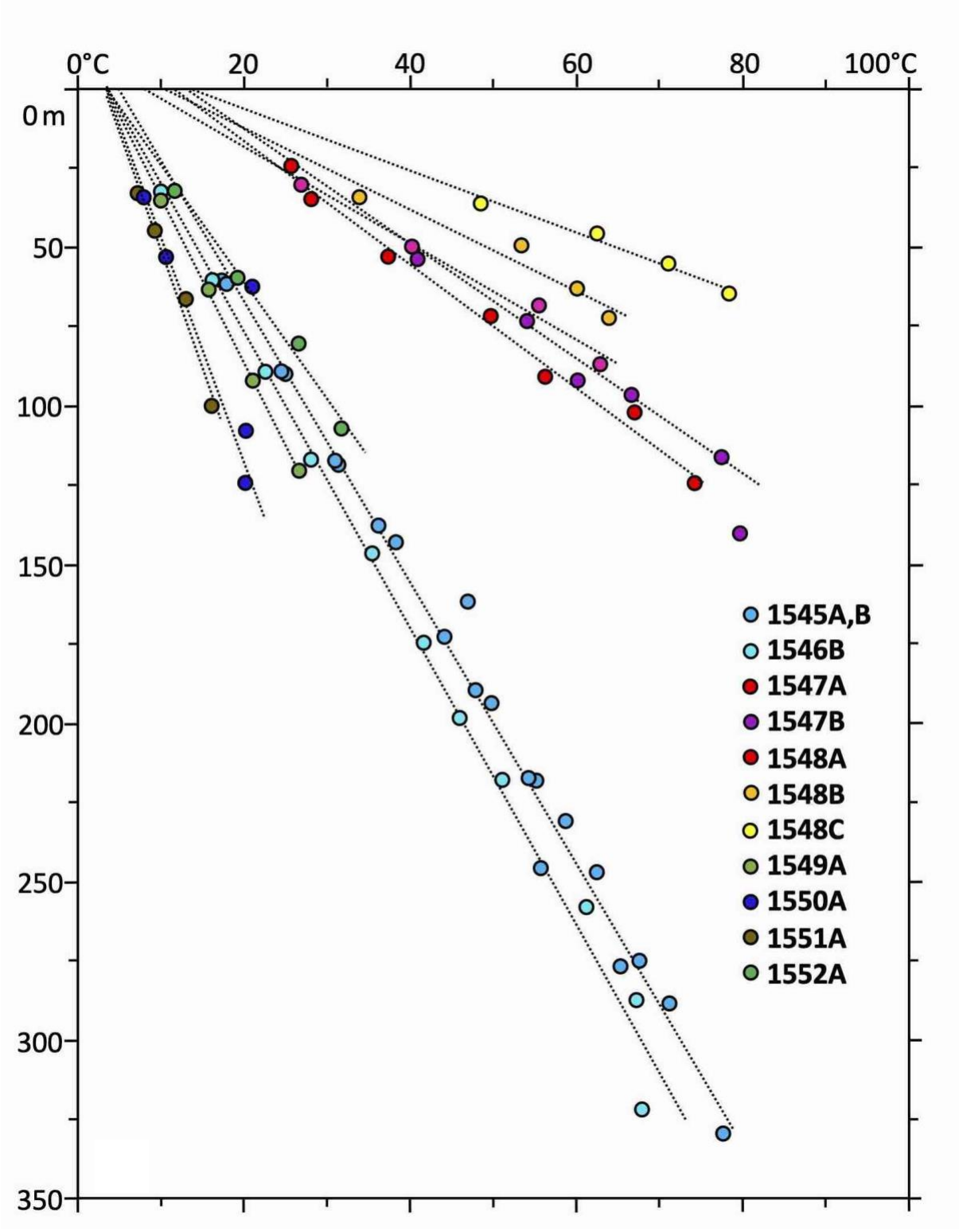

Figure 2. Temperature profiles of Guaymas drilling sites, plotted from measurements tabulated in the site chapters of Expedition 385 (Teske et al. 2021c-h).

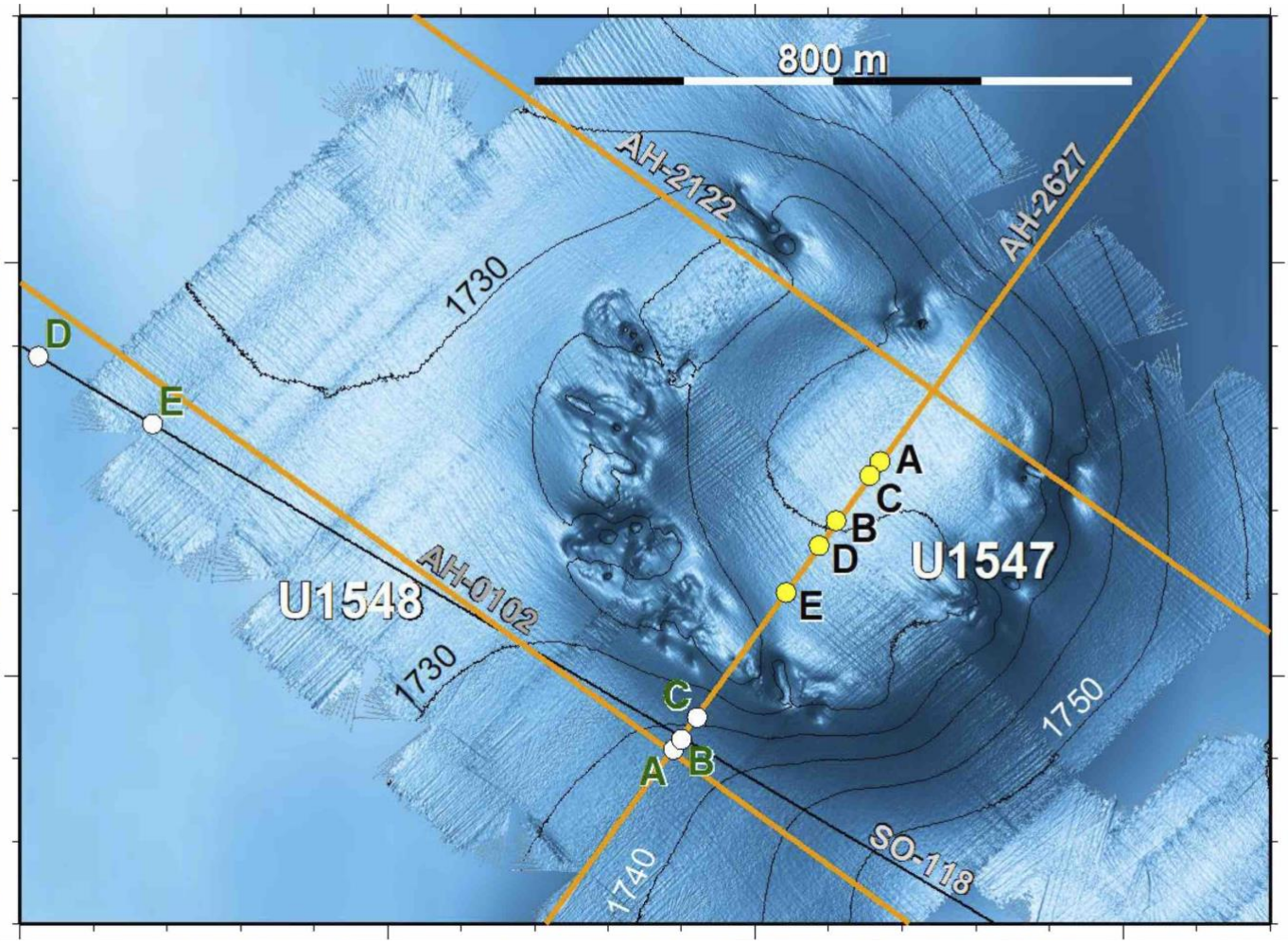

Figure 3. Ringvent Mound site with IODP Expedition 385 drilling sites and hole positions (U1547A-E and U1548A-E), and multichannel seismic lines for subsurface mapping (Teske et al. 2021d). The topographical high marks the edge of the shallow subsurface sill where hydrothermally circulating fluids reach the sediment surface. Sequence data from cores 1547B and 1548B represent the microbial communities within the interior sedimented bowl, and the hydrothermally impacted communities just outside the sill.

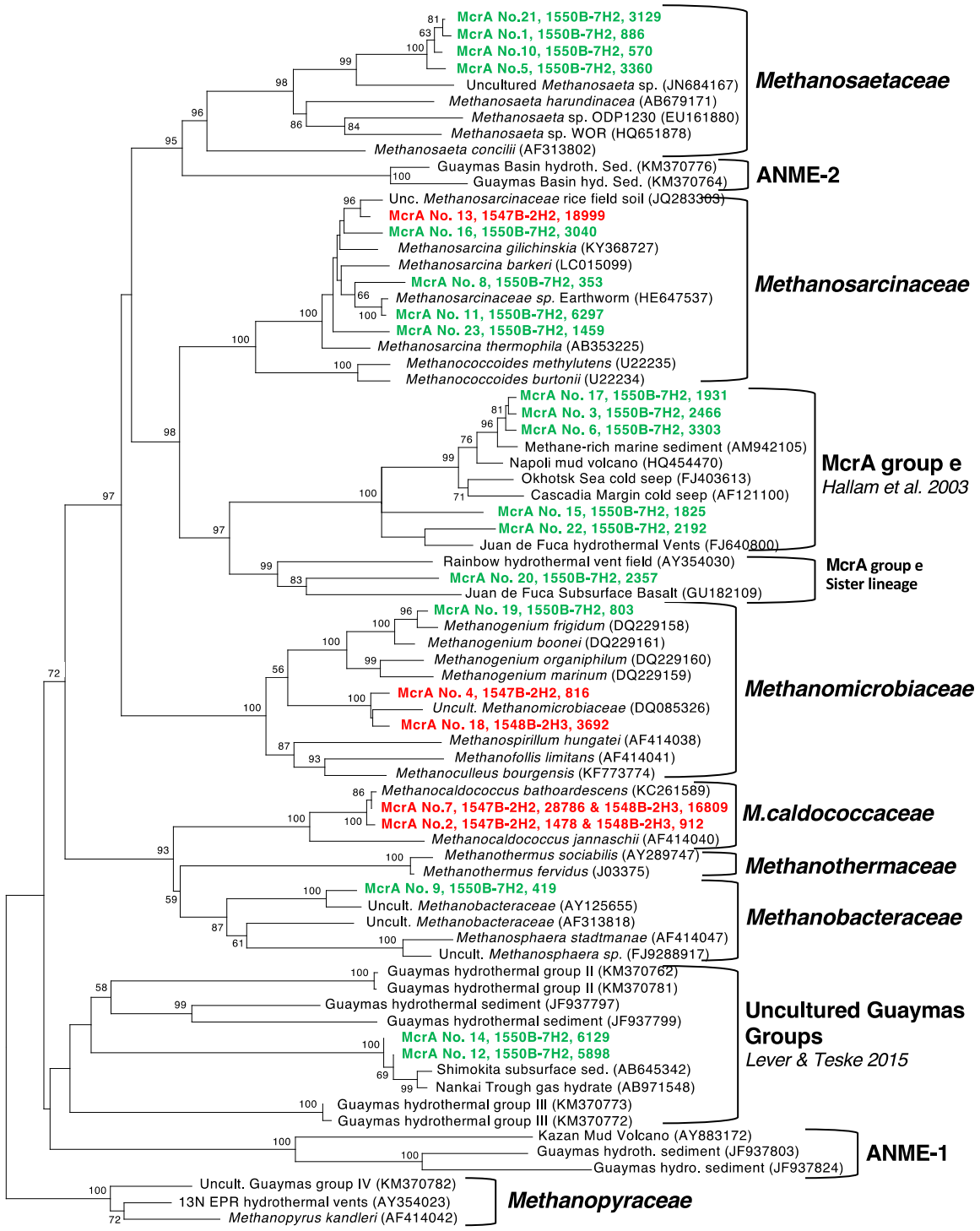

Figure 4. Phylogenetic diversity of methanogen lineages detected with general methanogen primers, resulting in 23 ASVs of partial *mcrA* gene sequences. The phylogeny was constructed using the minimum evolution method of phylogenetic inference and included bootstrap values >

50%. ASVs from Ringvent sites U1547B and U1548B are plotted in red, and ASVs from axial site 1550B are plotted in green. Each taxon label starts with the ASV number, followed by the IODP sample code (drilling site, subcore number and segment), and the number of sequences within each ASV. *Methanocaldococcaceae* ASVs No. 2 and 7 were recovered from both samples each, U1547_2H2 and U1548_2H2.

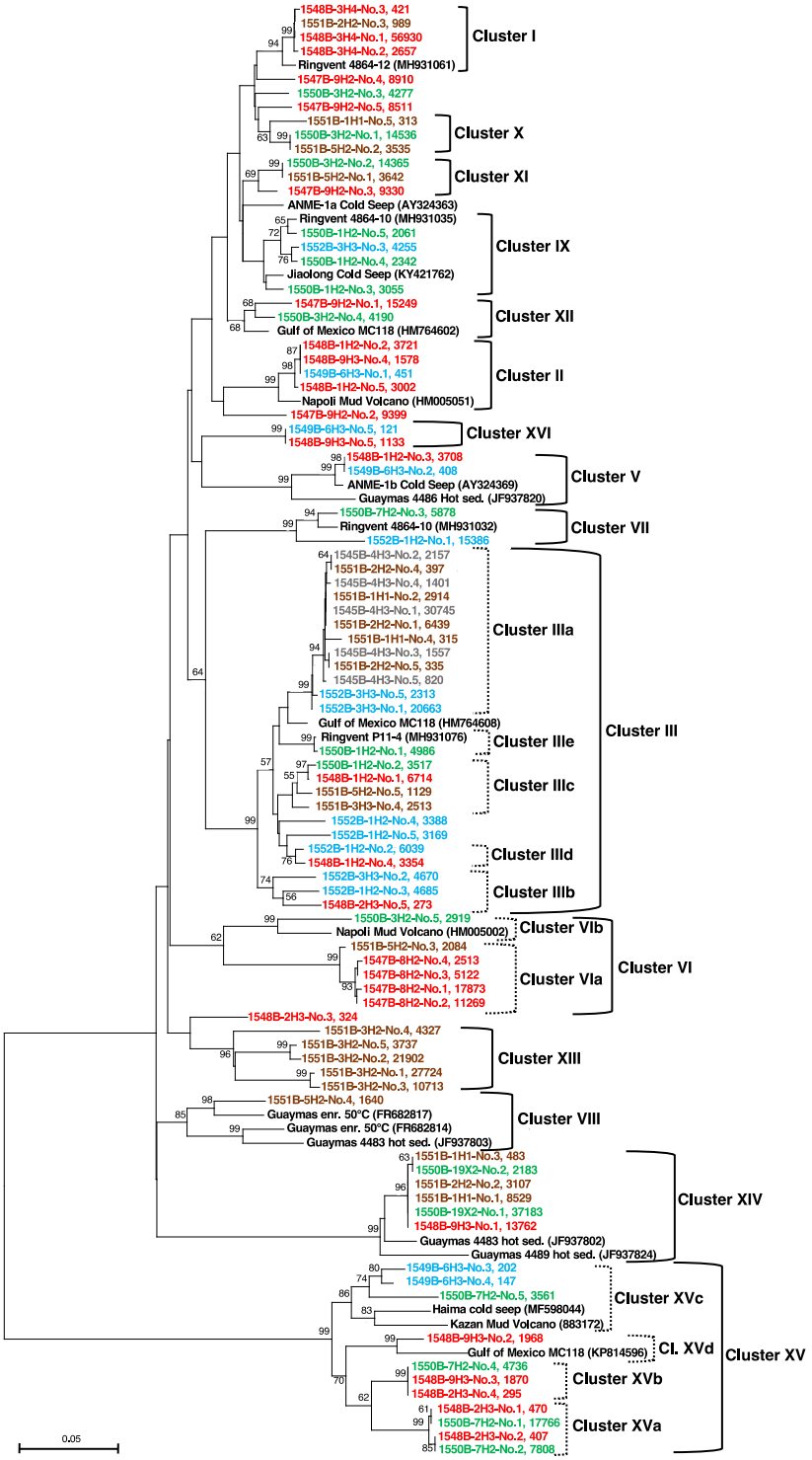
1548B-3H4-No.3, 421
1551B-2H2-No.3, 989
1548B-3H4-No.1, 56930
1548B-3H4-No.2, 2657
Ringvent 4864-12 (MH931061)
Cluster I
1547B-9H2-No.4, 8910
1550B-3H2-No.3, 4277
1547B-9H2-No.5, 8511
1551B-1H1-No.5, 313
1550B-3H2-No.1, 14536
1551B-5H2-No.2, 3535
Cluster X
1550B-3H2-No.2, 14365
1551B-5H2-No.1, 3642
1547B-9H2-No.3, 9330
Cluster XI
ANME-1a Cold Seep (AY324363)
Ringvent 4864-10 (MH931035)
1550B-1H2-No.5, 2061
1552B-3H3-No.3, 4255
1550B-1H2-No.4, 2342
Jiaolong Cold Seep (KY421762)
1550B-1H2-No.3, 3055
Cluster IX
1547B-9H2-No.1, 15249
1550B-3H2-No.4, 4190
Gulf of Mexico MC118 (HM764602)
Cluster XII
1548B-1H2-No.2, 3721
1548B-9H3-No.4, 1578
1549B-6H3-No.1, 451
1548B-1H2-No.5, 3002
Napoli Mud Volcano (HM005051)
Cluster II
1547B-9H2-No.2, 9399
1549B-6H3-No.5, 121
1548B-9H3-No.5, 1133
Cluster XVI
1548B-1H2-No.3, 3708
1549B-6H3-No.2, 408
ANME-1b Cold Seep (AY324369)
Guaymas 4486 Hot sed. (JF937820)
Cluster V
1550B-7H2-No.3, 5878
Ringvent 4864-10 (MH931032)
1552B-1H2-No.1, 15386
Cluster VII
1545B-4H3-No.2, 2157
1551B-2H2-No.4, 397
1545B-4H3-No.4, 1401
1551B-1H1-No.2, 2914
1545B-4H3-No.1, 30745
1551B-2H2-No.1, 6439
1551B-1H1-No.4, 315
1545B-4H3-No.3, 1557
1551B-2H2-No.5, 335
1545B-4H3-No.5, 820
1552B-3H3-No.5, 2313
1552B-3H3-No.1, 20663
Cluster IIIa
Gulf of Mexico MC118 (HM764608)
Ringvent P11-4 (MH931076)
1550B-1H2-No.1, 4986
Cluster IIIe
1550B-1H2-No.2, 3517
1548B-1H2-No.1, 6714
1551B-5H2-No.5, 1129
1551B-3H3-No.4, 2513
Cluster IIIc
1552B-1H2-No.4, 3388
1552B-1H2-No.5, 3169
1552B-1H2-No.2, 6039
1548B-1H2-No.4, 3354
Cluster IIId
1552B-3H3-No.2, 4670
1552B-1H2-No.3, 4685
1548B-2H3-No.5, 273
Cluster IIIb
Cluster III
1550B-3H2-No.5, 2919
Napoli Mud Volcano (HM005002)
Cluster VIb
1551B-5H2-No.3, 2084
1547B-8H2-No.4, 2513
1547B-8H2-No.3, 5122
1547B-8H2-No.1, 17873
1547B-8H2-No.2, 11269
Cluster VIa
Cluster VI
1548B-2H3-No.3, 324
1551B-3H2-No.4, 4327
1551B-3H2-No.5, 3737
1551B-3H2-No.2, 21902
1551B-3H2-No.1, 27724
1551B-3H2-No.3, 10713
Cluster XIII
1551B-5H2-No.4, 1640
Guaymas enr. 50°C (FR682817)
Guaymas enr. 50°C (FR682814)
Guaymas 4483 hot sed. (JF937803)
Cluster VIII
1551B-1H1-No.3, 483
1550B-19X2-No.2, 2183
1551B-2H2-No.2, 3107
1551B-1H1-No.1, 8529
1550B-19X2-No.1, 37183
1548B-9H3-No.1, 13762
Guaymas 4483 hot sed. (JF937802)
Guaymas 4489 hot sed. (JF937824)
Cluster XIV
1549B-6H3-No.3, 202
1549B-6H3-No.4, 147
1550B-7H2-No.5, 3561
Haima cold seep (MF598044)
Kazan Mud Volcano (883172)
Cluster XVc
1548B-9H3-No.2, 1968
Gulf of Mexico MC118 (KP814596)
Cl. XVd
1550B-7H2-No.4, 4736
1548B-9H3-No.3, 1870
1548B-2H3-No.4, 295
Cluster XVb
1548B-2H3-No.1, 470
1550B-7H2-No.1, 17766
1548B-2H3-No.2, 407
1550B-7H2-No.2, 7808
Cluster XVa
Cluster XV
0.05

409

Figure 5. General ANME-1 minimum evolution phylogeny based on partial *mcrA* gene sequences, encompassing the five most frequently recovered ASVs from each drilling site and sample. Reference site U1545 sequences are plotted in grey, those from Ringvent sites U1547B and U1548B are plotted in red, axial site U1550B sequences appear in green, terrestrial site U1551B sequences in brown, and seep site U1549B and U1552B sequences are plotted in blue. Each taxon label starts with the IODP sample code (drilling site, subcore number and segment), followed by the ASV number and the number of sequences within each ASV. Site-specific phylogenies that include a greater number of ASVs (more than five) for each site are available as Supplemental Figures S2 to S6.

Figure 6. Abundance dot plot of mcrA gene amplicons (represented by > 1000 sequences) color-coded by site, as in Figures 1, 4 and 5. Dot size indicates number of sequences. X-axis indicates the samples. The Y-axis indicates the *mcrA* sequences and their clustering. A version with full sample annotation on the left margin is available as Supplementary Figure S8.

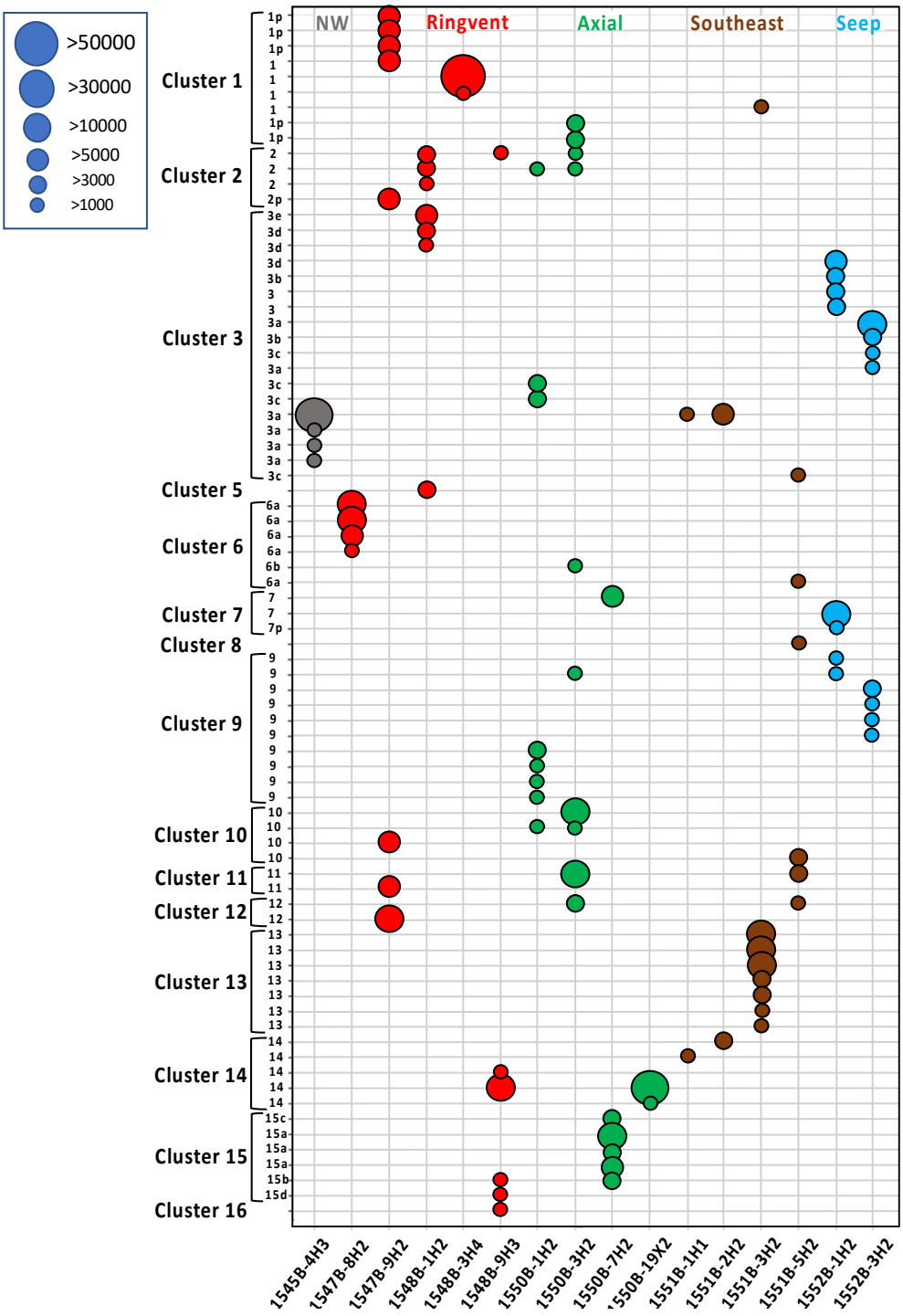
>50000
>30000
>10000
>5000
>3000
>1000
NW
Ringvent
Axial
Southeast
Seep
Cluster 1
Cluster 2
Cluster 3
Cluster 5
Cluster 6
Cluster 7
Cluster 8
Cluster 9
Cluster 10
Cluster 11
Cluster 12
Cluster 13
Cluster 14
Cluster 15
Cluster 16
1545B-4H3
1547B-8H2
1547B-9H2
1548B-1H2
1548B-3H4
1548B-9H3
1550B-1H2
1550B-3H2
1550B-7H2
1550B-19X2
1551B-1H1
1551B-2H2
1551B-3H2
1551B-5H2
1552B-1H2
1552B-3H2

424

REFERENCES

1. Announcement of the Non-Renewal of the JOIDES Resolution Operations and Maintenance Cooperative Agreement. 2023. National Science Foundation. https://www.nsf.gov/news/news_summ.jsp?cntn_id=306986&org=OCE
2. Benito-Merino D, Zehnle H, Teske AP, Wegener G. 2022. Deep-branching ANME-1c archaea grow at the upper temperature limit of anaerobic oxidation of methane. *Front Microbiol*. 13:988871; https://doi.org/10.3389/fmicb.2022.988871
3. Bojanova DP, De Anda VY, Haghnegahdar MA, Teske AP, Ash JL, Young ED, Baker BJ, LaRowe DE, Amend JP, and IODP Expedition Scientists. 2023. Well-hidden Methanogenesis in deep, organic-rich sediments of Guaymas Basin, Gulf of California. *ISME J.* https://doi.org/10.1038/s41396-023-01485-y
4. Bolyen E, Rideout JR, Dillon MR, Bokulich NA, Abnet CC, Al-Ghalith GA, Alexander H, Alm EJ, Arumugam M, Asnicar F, Bai Y, Bisanz JE, Bittinger K, Brejnrod A, Brislawn CJ, Brown CT, Callahan BJ, Caraballo-Rodríguez AM, Chase J, Cope EK, Da Silva R, Diener C, Dorrestein PC, Douglas GM, Durall DM, Duvallet C, Edwardson CF, Ernst M, Estaki M, Fouquier J, Gauglitz JM, Gibbons SM, Gibson DL, Gonzalez A, Gorlick K, Guo J, Hillmann B, Holmes S, Holste H, Huttenhower C, Huttley GA, Janssen S, Jarmusch AK, Jiang L, Kaehler BD, Kang KB, Keefe CR, Keim P, Kelley ST, Knights D, Koester I, Kosciolek T, Kreps J, Langille MGI, Lee J, Ley R, Liu YX, Loftfield E, Lozupone C, Maher M, Marotz C, Martin BD, McDonald D, McIver LJ, Melnik AV, Metcalf JL, Morgan SC, Morton JT, Naimey AT, Navas-Molina JA, Nothias LF, Orchanian SB, Pearson T, Peoples SL, Petras D, Preuss ML, Pruesse E, Rasmussen LB, Rivers A, Robeson MS 2nd, Rosenthal P, Segata N, Shaffer M, Shiffer A, Sinha R, Song

SJ, Spear JR, Swafford AD, Thompson LR, Torres PJ, Trinh P, Tripathi A, Turnbaugh PJ, Ul-Hasan S, van der Hooft JJJ, Vargas F, Vázquez-Baeza Y, Vogtmann E, von Hippel M, Walters W, Wan Y, Wang M, Warren J, Weber KC, Williamson CHD, Willis AD, Xu ZZ, Zaneveld JR, Zhang Y, Zhu Q, Knight R, Caporaso JG. 2019. Reproducible, interactive, scalable, and extensible microbiome data science using QIIME 2. *Nat. Biotechnol*. **37**, 852–857. https://doi.org/10.1038/s41587-019-0209-9

5. Biddle JF, Cardman Z, Mendlovitz H, *et al*. 2012. Anaerobic oxidation of methane at different temperature regimes in Guaymas Basin hydrothermal sediments. *ISME J*. **6**:1018–1031. https://doi.org/10.1038/ismej.2011.164
6. Pérez Castro S, Borton MA, Regan K, Hrabe de Angelis I, Wrighton KC, Teske AP, Strous M, Ruff SE. 2021. Degradation of biological macromolecules supports uncultured microbial populations in Guaymas Basin hydrothermal sediments. *ISME J*. **15**, 3480–3497. https://doi.org/10.1038/s41396-021-01026-5
7. Dhillon A, Lever M, Lloyd KG, Albert DB, Sogin ML, Teske AP. 2005. Methanogen diversity evidenced by molecular characterization of methyl coenzyme M reductase A (mcrA) genes in hydrothermal sediments of the Guaymas Basin. *Appl Environ Microbiol*. **71**:4592–4601. https://doi.org/10.1128/AEM.71.8.4592-4601.2005
8. Dowell F, Cardman Z, Dasarathy S, Kellermann MY, McKay LJ, MacGregor BJ, Ruff SE, Biddle JF, Lloyd KG, Lipp JS, Hinrichs K-U, Albert DB, Mendlovitz H, Teske A. 2016 Microbial communities in methane and short alkane-rich hydrothermal sediments of Guaymas Basin. *Front Microbiol* 7:17. https://doi.org/10.3389/fmicb.2016.00017
9. Hallam SJ, Girguis PR, Preston CM, Richardson PM, DeLong EF. 2003. Identification of methyl coenzyme M reductase A (mcrA) genes associated with methane-oxidizing

archaea. *Appl Environ Microbiol*. **69**:5483-5491. https://doi.org/10.1128/AEM.69.9.5483-5491.2003

10. Heesemann M, Villinger H, Fisher AT, Tréhu AM, White S. 2006. Data report: testing and deployment of the new APCT-3 tool to determine in situ temperatures while piston coring. In Riedel, M., Collett, T.S., Malone, M.J., and the Expedition 311 Scientists. *Proc. IODP*, **311**: Washington, DC (Integrated Ocean Drilling Program Management International, Inc.). https://doi.org/10.2204/iodp.proc.311.108.2006
11. Holler T, Widdel F, Knittel K, Amann R, Kellermann MY, Hinrichs KU, Teske AP, Boetius A, Wegener G. 2011. Thermophilic anaerobic oxidation of methane by marine microbial consortia. *ISME J*. **5**:1946–1956. https://doi.org/10.1038/ismej.2011.77
12. Integrated Ocean Drilling Program 2011. IODP Depth Scales terminology. Available online at. https://www.iodp.org/policies-and-guidelines/142-iodp-depth-scales-terminology-april-2011/file
13. Jones WJ, Leigh JA, Mayer F, Woese CR, Wolfe RS. 1983. *Methanococcus jannaschii* sp. nov., an extremely thermophilic methanogen from a submarine hydrothermal vent. *Arch Microbiol*. **136**:254–261. https://doi.org/10.1007/BF00425213
14. Kurr M, Huber R, König H, Jannasch HW, Fricke H, Trincone A, Kristjansson JK, and Stetter KO. 1991. *Methanopyrus kandleri*, gen. and sp. nov. represents a novel group of hyperthermophilic methanogens, growing at 110°C. *Arch. Microbiol*. **156**:239 –247. https://doi.org/10.1007/BF00262992
15. Laso-Pérez R, Wu F, Crémière A, *et al*. 2023. Evolutionary diversification of methanotrophic Ca. Methanophagales (ANME-1) and their expansive virome. *Nat Microbiol*. **8**:231-245. https://doi.org/10.1038/s41564-022-01297-4

16. Lazar CS, L'Haridon S, Pignet P, Toffib L. 2011. Archaeal Populations in Hypersaline Sediments Underlying Orange Microbial Mats in the Napoli Mud Volcano. *Appl Environ Microbiol*. **77**(9):3120–3131. https://doi.org/10.1128/AEM.01296-10

17. Lever MA, Teske AP. 2015. Diversity of Methane-Cycling Archaea in Hydrothermal Sediment Investigated by General and Group-Specific PCR Primers. *Appl Environ Microbiol*. **81**(4):1426–1441. https://doi.org/10.1128/AEM.03588-14

18. Lin YS, Koch BP, Feseker T, Ziervogel K, Goldhammer T, Schmidt F, Witt M, Kellermann MY, Zabel M, Teske AP, Hinrichs KU. 2017. Near-surface Heating of Young Rift Sediment Causes Mass Production and Discharge of Reactive Dissolved Organic Matter. *Sci Reports*. **7**:44864. https://doi.org/10.1038/srep44864

19. Liu Y, Whitman WB. 2008. Metabolic, phylogenetic, and ecological diversity of the methanogenic archaea. *Ann N Y Acad Sci*. **1125**. https://doi.org/10.1196/annals.1419.019

20. Lizarralde D, Teske A, Höfig TW, González-Fernández A, the IODP Expedition 385 Scientists. 2023. Carbon released by sill intrusion into young sediments measured through scientific drilling. Geology. **51**(4): 329-333. https://doi.org/10.1130/G50665.1

21. Luton PE, Wayne JM, Sharp RJ, Riley PW. 2002. The mcrA gene as an alternative to 16S rRNA in the phylogenetic analysis of methanogen populations in landfill. *Microbiology* **148**, 3521–3530. https://doi.org/10.1099/00221287-148-11-3521

22. Mara P, Zhou Y, Teske AP, Morono Y, Beaudoin D, Edgcomb VP. Microbial gene expression in Guaymas Basin subsurface sediments responds to hydrothermal stress and energy limitation. *ISME J*., https://doi.org/10.1038/s41396-023-01492-z.

23. McKay LJ, Klokman VW, Mendlovitz HP, LaRowe DE, Hoer DR, Albert D, Amend JP, Teske AP. 2016. Thermal and geochemical influences on microbial biogeography in the

hydrothermal sediments of Guaymas Basin, Gulf of California. *Environ. Microbiol. Rep.* **8**(1):150–161. https://doi.org/10.1111/1758-2229.12365

24. NCBI Resource Coordinators, Database resources of the National Center for Biotechnology Information, Nucleic Acids Research, **42**(D1): D7–D17. https://doi.org/10.1093/nar/gkt1146
25. Neumann F, Negrete-Aranda R, Harris RN, Contreras J, Galerne C, Peña-Salinas MS, Splez RM, Teske AP, Lizarralde D, Höfig TW, Expedition Scientists. 2023. Heat flow and thermal regime in the Guaymas Basin, Gulf of California: Estimates of conductive and advective heat transport. *Basin Research* **35**:1308-1328; https://doi.org/10.1111/bre.12755
26. Nobu MK., Narihiro T, Kuroda K, Mei R, Liu WT. 2016. Chasing the elusive Euryarchaeota class WSA2: genomes reveal a uniquely fastidious methyl-reducing methanogen. *ISME J.* 10, 2478–2487. https://doi.org/10.1038/ismej.2016.33
27. Oremland RS., Culbertson C, Simoneit BRT. 1982. Methanogenic activity in sediment from Leg 64, Gulf of California. In Curray JR, Moore DG, et al., *Initial Reports of the Deep Sea Drilling Project*, 64: Washington, DC (U.S. Government Printing Office), 759–762. https://doi.org/10.2973/dsdp.proc.64.122.1982
28. Persad LD, Marsaglia KM. 2023. Data Report: Detailed lithologic columns for IODP Expeditions 385 and DSDP Leg 64 Sites in the Guaymas Basin, Gulf of California, Mexico. In Teske A, Lizarralde D, Höfig TW, and the Expedition 385 Scientists, Guaymas Basin Tectonics and Biosphere. Proceedings of the International Ocean Discovery Program, 385: College Station, TX (International Ocean Discovery Program). https://doi.org/10.14379/iodp.proc.385.202.2023

29. Ramírez GA, Mara P, Sehein T, Wegener G, Chambers CR, Joye SB, Peterson RN, Philippe A, Burgard G, Edgcomb VP, Teske AP. (2021) Environmental factors shaping bacterial, archaeal and fungal community structure in hydrothermal sediments of Guaymas Basin, Gulf of California. *PLoS ONE* **16**(9): e0256321. https://doi.org/10.1371/journal.pone.0256321

30. Rattray JE, Chakraborty A, Elizondo G, Ellefson E, Bernard B, Brooks J, Hubert CRJ. 2022. Endospores associated with deep seabed geofluid features in the eastern Gulf of Mexico. *Geobiology* **20**(6):823–836. https://doi.org/10.1111/gbi.12517

31. Simoneit BRT, Summerhayes CP, Meyers PA. 1986. Sources and hydrothermal alteration of organic matter in Quaternary sediments: a synthesis of studies from the Central Gulf of California. *Marine and Petroleum Geology* **3**(4):282–297. https://doi.org/10.1016/0264-8172(86)90033-4

32. Speth DR, Yu FB, Connon SA, Lim S, Magyar JS, Pena-Salinas ME, Quake, S.R., Orphan, V.J., 2022. Microbial communities of Auka hydrothermal sediments shed light on vent biogeography and the evolutionary history of thermophily. *ISME J*. **16**, 1750–1764. https://doi.org/10.1038/s41396-022-01222-x

33. Stewart LC, Jung JH, Kim YT, Kwon SW, Park CS, Holden JF 2015. *Methanocaldococcus bathoardescens* sp. nov., a hyperthermophilic methanogen isolated from a volcanically active deep-sea hydrothermal vent. *Int J Syst Evol Microbiol*. **65**:1280-1283. https://doi.org/10.1099/ijs.0.000097

34. Teske AP, McKay LJ, Ravelo AC, Aiello I, Mortera C, Núńez-Useche F, Canet C, Chanton JP, Brunner B, Hensen C, Ramírez GA, Sibert RJ, Turner T, White D, Chambers CR, Buckley A, Joye SB, Soule SA, Lizarralde D. 2019. Characteristics and Evolution of

sill-driven off-axis hydrothermalism in Guaymas Basin – the Ringvent site. *Sci Reports*. **9**:13847. https://doi.org/10.1038/s41598-019-50200-5

35. Teske A, Lizarralde D, Höfig TW, Aiello IW, Ash JL, Bojanova DP, Buatier MD, Edgcomb VP, Galerne CY, Gontharet S, Heuer VB, Jiang S, Kars MAC, Khogenkumar Singh S, Kim JH, Koornneef LMT, Marsaglia KM, Meyer NR, Morono Y, Negrete-Aranda R, Neumann F, Pastor LC, Peña-Salinas ME, Perez-Cruz LL, Ran L, Riboulleau A, Sarao JA, Schubert F, Stock JM,Toffin LMAA, Xie W, Yamanaka T, Zhuang G. 2021a. Expedition summary. *In* Teske A, Lizarralde, D, Höfig TW, and the Expedition 385 Scientists, *Guaymas Basin Tectonics and Biosphere*. Proceedings of the International Ocean Discovery Program, 385: College Station, TX (International Ocean Discovery Program). https://doi.org/10.14379/iodp.proc.385.101.2021

36. Teske A, Lizarralde D, Höfig TW, Aiello IW, Ash JL, Bojanova DP, Buatier MD, Edgcomb VP, Galerne CY, Gontharet S, Heuer VB, Jiang S, Kars MAC, Khogenkumar Singh S, Kim JH, Koornneef LMT, Marsaglia KM, Meyer NR, Morono Y, Negrete-Aranda R, Neumann F, Pastor LC, Peña-Salinas ME, Perez-Cruz LL, Ran L, Riboulleau A, Sarao JA, Schubert F, Stock JM,Toffin LMAA, Xie W, Yamanaka T, Zhuang G. 2021b. Site U1545. *In* Teske A, Lizarralde D, Höfig TW, and the Expedition 385 Scientists, *Guaymas Basin Tectonics and Biosphere*. Proceedings of the International Ocean Discovery Program, 385: College Station, TX (International Ocean Discovery Program). https://doi.org/10.14379/iodp.proc.385.103.2021

37. Teske A, Lizarralde D, Höfig TW, Aiello IW, Ash JL, Bojanova DP, Buatier MD, Edgcomb VP, Galerne CY, Gontharet S, Heuer VB, Jiang S, Kars MAC, Khogenkumar Singh S, Kim JH, Koornneef LMT, Marsaglia KM, Meyer NR, Morono Y, Negrete-Aranda R, Neumann

F, Pastor LC, Peña-Salinas ME, Perez-Cruz LL, Ran L, Riboulleau A, Sarao JA, Schubert F, Stock JM,Toffin LMAA, Xie W, Yamanaka T, Zhuang G. 2021c. Site U1546. *In* Teske A, Lizarralde D, Höfig TW, and the Expedition 385 Scientists, *Guaymas Basin Tectonics and Biosphere*. Proceedings of the International Ocean Discovery Program, 385: College Station, TX (International Ocean Discovery Program). https://doi.org/10.14379/iodp.proc.385.104.2021

38. Teske A, Lizarralde D, Höfig TW, Aiello IW, Ash JL, Bojanova DP, Buatier MD, Edgcomb VP, Galerne CY, Gontharet S, Heuer VB, Jiang S, Kars MAC, Khogenkumar Singh S, Kim JH, Koornneef LMT, Marsaglia KM, Meyer NR, Morono Y, Negrete-Aranda R, Neumann F, Pastor LC, Peña-Salinas ME, Perez-Cruz LL, Ran L, Riboulleau A, Sarao JA, Schubert F, Stock JM,Toffin LMAA, Xie W, Yamanaka T, Zhuang G. 2021d. Sites U1547 and U1548. *In* Teske A, Lizarralde D, Höfig TW, and the Expedition 385 Scientists, *Guaymas Basin Tectonics and Biosphere*. Proceedings of the International Ocean Discovery Program, 385: College Station, TX (International Ocean Discovery Program). https://doi.org/10.14379/iodp.proc.385.105.2021

39. Teske A, Lizarralde D, Höfig TW, Aiello IW, Ash JL, Bojanova DP, Buatier MD, Edgcomb VP, Galerne CY, Gontharet S, Heuer VB, Jiang S, Kars MAC, Khogenkumar Singh S, Kim JH, Koornneef LMT, Marsaglia KM, Meyer NR, Morono Y, Negrete-Aranda R, Neumann F, Pastor LC, Peña-Salinas ME, Perez-Cruz LL, Ran L, Riboulleau A, Sarao JA, Schubert F, Stock JM,Toffin LMAA, Xie W, Yamanaka T, Zhuang G. 2021e. Site U1549. *In* Teske A, Lizarralde D, Höfig TW, and the Expedition 385 Scientists, *Guaymas Basin Tectonics and Biosphere*. Proceedings of the International Ocean Discovery Program, 385: College

Station, TX (International Ocean Discovery Program). https://doi.org/10.14379/iodp.proc.385.106.2021

40. Teske A, Lizarralde D, Höfig TW, Aiello IW, Ash JL, Bojanova DP, Buatier MD, Edgcomb VP, Galerne CY, Gontharet S, Heuer VB, Jiang S, Kars MAC, Khogenkumar Singh S, Kim JH, Koornneef LMT, Marsaglia KM, Meyer NR, Morono Y, Negrete-Aranda R, Neumann F, Pastor LC, Peña-Salinas ME, Perez-Cruz LL, Ran L, Riboulleau A, Sarao JA, Schubert F, Stock JM,Toffin LMAA, Xie W, Yamanaka T, Zhuang G. 2021f. Site U1550. *In* Teske A, Lizarralde D, Höfig TW, and the Expedition 385 Scientists, *Guaymas Basin Tectonics and Biosphere*. Proceedings of the International Ocean Discovery Program, 385: College Station, TX (International Ocean Discovery Program). https://doi.org/10.14379/iodp.proc.385.107.2021

41. Teske A, Lizarralde D, Höfig TW, Aiello IW, Ash JL, Bojanova DP, Buatier MD, Edgcomb VP, Galerne CY, Gontharet S, Heuer VB, Jiang S, Kars MAC, Khogenkumar Singh S, Kim JH, Koornneef LMT, Marsaglia KM, Meyer NR, Morono Y, Negrete-Aranda R, Neumann F, Pastor LC, Peña-Salinas ME, Perez-Cruz LL, Ran L, Riboulleau A, Sarao JA, Schubert F, Stock JM,Toffin LMAA, Xie W, Yamanaka T, Zhuang G. 2021g. Site U1551. *In* Teske A, Lizarralde D, Höfig TW, and the Expedition 385 Scientists, *Guaymas Basin Tectonics and Biosphere*. Proceedings of the International Ocean Discovery Program, 385: College Station, TX (International Ocean Discovery Program). https://doi.org/10.14379/iodp.proc.385.108.2021

42. Teske A, Lizarralde D, Höfig TW, Aiello IW, Ash JL, Bojanova DP, Buatier MD, Edgcomb VP, Galerne CY, Gontharet S, Heuer VB, Jiang S, Kars MAC, Khogenkumar Singh S, Kim JH, Koornneef LMT, Marsaglia KM, Meyer NR, Morono Y, Negrete-Aranda R, Neumann

F, Pastor LC, Peña-Salinas ME, Perez-Cruz LL, Ran L, Riboulleau A, Sarao JA, Schubert F, Stock JM,Toffin LMAA, Xie W, Yamanaka T, Zhuang G. Site U1552. *In* Teske A, Lizarralde D, Höfig TW, and the Expedition 385 Scientists, *Guaymas Basin Tectonics and Biosphere*. Proceedings of the International Ocean Discovery Program, 385: College Station, TX (International Ocean Discovery Program). https://doi.org/10.14379/iodp.proc.385.109.2021

43. Teske, A, Wegener G., Chanton JP, White D, MacGregor BJ, Hoer D, de Beer D, Zhuang G, Saxton, MA, Joye SB, Lizarralde D, Soule SA, Ruff SE. 2021i. Microbial communities under distinct thermal and geochemical regimes in axial and off-axis sediments of Guaymas Basin. *Frontiers in Microbiology* 12:633649. https://doi.org/10.3389/fmicb.2021.633649

44. Thauer RK. 2019. Methyl (Alkyl)-Coenzyme M Reductases: Nickel F-430-Containing Enzymes Involved in Anaerobic Methane Formation and in Anaerobic Oxidation of Methane or of Short Chain Alkanes. *Biochemistry* **58**:5198-5220. https://doi.org/10.1021/acs.biochem.9b00164

45. Torres ME, Kim J-H. 2022. Data report: concentration and carbon isotopic composition in pore fluids from IODP Expedition 385. In Teske A, Lizarralde D, Höfig TW, and the Expedition 385 Scientists, Guaymas Basin Tectonics and Biosphere. Proceedings of the International Ocean Discovery Program, 385: College Station, TX (International Ocean Discovery Program). http://doi.org/10.14379/iodp.proc.385.201.2022

46. Underwood S, Lapham L, Teske A, Lloyd KG. 2016. Microbial community structure and methane-cycling activity of subsurface sediments at Mississippi Canyon 118 before the

Deepwater Horizon Disaster. *Deep-Sea Research II* **129**:148-156. https://doi.org/10.1016/j.dsr2.2015.01.011

47. Wegener G, Krukenberg V, Riedel D, Tegetmeyer HE, Boetius A. 2015. Intracellular wiring enables electron transfer between methanotrophic archaea and bacteria. *Nature* **526**:587–590.

48. Wellsbury P, Goodman K, Bart T, Cragg BA, Barnes SP, Parkes RJ. 1997. Deep marine biosphere fueled by increasing organic matter availability during burial and heating. *Nature*. **388**:573–576. https://doi.org/10.1038/41544